2 Photo-electrical properties of self-assembled photosystem I monolayers

In this chapter, PSI was immobilized on a gold surface with two linker molecules, i.e. 2-mercaptoethanol (2ME) and 3-mercapto-1-propanesulfonate (MPS). Through AFM measurements it was demonstrated that these molecules orient PSI trimer molecules on average in opposite directions. Via macroscopic electrical transport measurements, the absolute configuration of the PSI molecules on the surface was determined since it was that the mechanism of charge transport occurs via tunnelling. This finding suggests that the electron transport chain is not involved in electron transport. Hence the conductivity through PSI is dominated by the intrinsic dipole of PSI. Besides looking at electron transport in the dark, light experiments with AFM were performed on single PSI trimers. In contrast to experiments in the dark, no semiconducting I-V curves were measured but curves with ohmic characteristics.

2.1 Introduction

From all light-active proteins found in Nature, protein complex Photosystem I (PSI) is a promising candidate for use in bio-electronics because of its unique property of inducing electron transfer upon light irradiation. This electron transfer process over the protein structure is exploited for biological growth in living organisms such as cyanobacteria, algae and plants. Isolated PSI protein complexes have already been applied in different environments and have showed promising performance and potential for use in solar cells[1], hydrogen production units[2], and spatial light modulation transmission films[3]. Physically, a PSI protein complex can be regarded as an electrical current rectifying diode because it features a directional electron transport chain functioning in the electron extraction process from the P700 reaction centre, located at the bottom of the PSI to the top ferredoxin docking side. These feature quality PSI as an unique and attractive protein biomaterial for studying its electrical properties by a variety of experimental techniques[4-14]. In this research project, we studied the entire PSI complex (not the RCI in isolation) containing electron transport chain, the light-harvesting system of chlorophylls, the reaction center and the protein scaffold that keeps it all together.

Isolated PSI complexes taken from the thermophilic cyanobacterium *T. Elongatus* have evolutionary formed a trimer structure in order to improve light absorption and stability under harsh conditions. The PSI monomer has a polar stroma and lumen as well as an apolar region in contact with the membrane. Its dimensions measure approximately 13 × 8 × 9 nm and it contains 96 light-sensitive chlorophyll *a* (Chl a) molecules that are densely packed in the protein scaffold to harvest light. In the complex, harvested photons induce charge separation by chlorophylls in P700 (a special pair of Chl *a* molecules). Then electron transfer occurs from the primary electron donor complex to the primary electron acceptor, to the ferredoxin docking region through the built-in electron transport chain phylloquinone, F_X, F_A and F_B (Fe_4S_4 clusters) (**Figure 2.1a**). The complex exhibits a photovoltage of around 1 V under illumination with an internal quantum efficiency close to unity.

PSI can be anchored in a "downwards" orientation in which the natural flow of photo-generated electrons is towards the electrode surface (F_B down), an "upwards" orientation where electrons flow in the opposite direction (P700 adjacent to the substrate), or with its electron transport vector parallel to the substrate (**Figure 2.1b**). This level of control over the orientation of the electron transport chain provides an opportunity to determine its role in the tunnelling transport through PSI with the help a self-assembly process rather than modifying the complexes themselves. The method of orientating PSI on metal and metal-oxide surfaces range from surface modification with different functional groups that interact electrostatically with different parts of the protein complex, to direct covalent attachment via introducing of cysteine mutants[7] and SAMs with different functional head groups[9, 12]. One can examine the orientation of the complexes in the monolayer with atomic force microscopy (AFM) images and conducting probe AFM (CP-AFM) I-V curves.

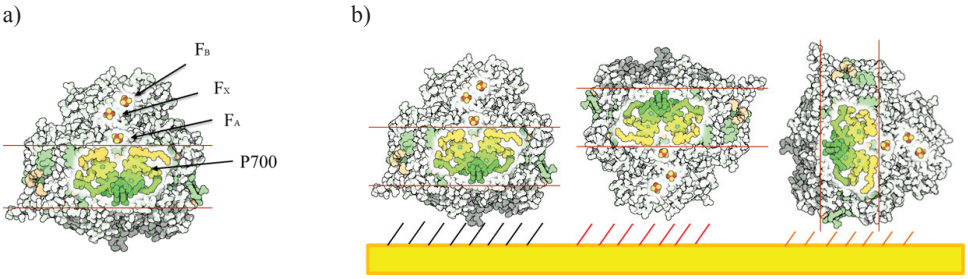

Figure 2.1 (a) Schematic representation of the electron transport chain in PSI (ET chain), F_A, F_X and F_B. (b) Possible orientations of PSI on Au surfaces induced by different chemical modification. Photosystem I can be oriented "upwards" (left) where the flow of electrons is from the surface (P700 adjacent to substrate), a "downwards" (middle) orientation in which the natural direction of the flow of electrons is towards the electrode surface (F_B down), or with its electron transport vector parallel (right) to the substrate.

Electron active proteins such as RCI, the PSI reaction centre (extracted from spinach) and full PSI protein complex (extracted from cyanobacterium, containing its own light harvesting system and charge separation reaction centre in the middle) are frequently used for device fabrication and all have different sizes and protein structures. According to previous reports on single RCI complexes, which are much smaller than the large multiprotein complex PSI, asymmetric charge transport is completely dependent on the orientation of RCI on an electrode's surface. Greenbaum et al.,[8-10] were the first to observe and explain this behaviour. They platinised one end of the photosynthetic complex directly on a surface and, during this process, the RCI complexes changed their initial orientation due to the electrostatic repulsion between positive charges on the non-platinized side of the RCI (the platinisation process can be only carried out at F_B protein side) and the positive charges present in the self-assembling monolayer on the gold surface[9]. They used scanning tunnelling spectroscopy (STS) to examine the electronic properties of each RCI, which elicited orientation-dependent I-V asymmetry. Others have subsequently observed this behaviour in RCIs as single complexes[11] and in SAMs[12]. This phenomenon is easily combined with light-driven processes[6], which involves hopping transport (to move through the transport chain as the electron changes in energy) and therefore should not play a role in tunnelling measurements. However, the absolute orientation of the RCI and, by extension, the PSI is determined by STS data based on the assumption that the direction of asymmetry (rectification) follows the electron transport chain.

It should be possible to understand the role of the electron transport chain in tunnelling currents using light experiments. Light-induced electrical currents should be enhanced in the direction of the electron transport chain or suppressed in the opposite direction. However, such light experiments employing single molecule techniques, in order to prove the role of the "*activated electron transport chain*", have not yet been carried out. The first illumination experiments, which deal with the rectification and role of the electron transport chain, demonstrated a new observation of ohmic I-V curves measured in the case of a single PSI photocurrent with the help

of scanning near optical microscopy (SNOM). The photocurrent produced by one PSI protein complex covalently attached to a gold surface was determined as the offset shift of the electrical current at zero applied bias[6]. However, the I-V characteristics recorded under dark conditions and their characteristic asymmetric behaviour due to their orientations were not reported for these SNOM experiments, which made it difficult to pinpoint the actual role of the active electron transport chain under illumination[6].

In this study, the electrical current rectification properties of PSI protein complexes have been investigated using CP-AFM and EGaIn. The latter technique uses a small drop of liquid metal consisting of an eutectic mixture of Gallium and Indium to probe the electrical properties of a surface of molecules assembled at a metal substrate[15, 16]. Both techniques have been employed to investigate the physical properties of the PSI in absence of light irradiation regarding its conducting properties through a single protein and protein monolayers. The temperature dependent tunnelling currents measured, clearly demonstrated its "*non-hopping*" nature. The conductivity of light-generated electrons via the built-in transport chain should be a hopping process. Rectification as a result of the PSI neutral dipole moment was proposed to explain the asymmetric tunnelling current based on the dipole moment of the electrical field formed locally within the PSI due to the protein scaffold. Additionally, we observed that the I-V characteristics changed from "semiconducting" to "ohmic" behaviours under illumination, which has not been reported before in the literature. The observed transition in conductivity limits the application of the I-V rectification scenario as a tool for determining the orientation of photosynthetic proteins under illumination. The light-generated electrons under illumination do not influence the symmetry of the measured I-V curves in CP-AFM at positive and negative applied biases *i.e.* its enhancement. This can be explained by the fact that the light induced electrons at the P700 reaction centre of the PSI are powered by an applied external electrical field between the metal surface and the CP-AFM conducting probe, but not by the electron acceptor transport pathway built into the protein scaffold.

2.2 Characterization of PSI proteins with conducting AFM

We exposed ultra-flat template-stripped Au (AuTS) substrates to a solution of 1 mM 2-mercaptoethanol (2ME)[9] or sodium 3-mercapto-1-propanesulfonate (MPS)[17] to form "director SAMs" to bias the orientation of PSI trimers that self-assemble on top of these SAMs.[12] These director SAMs differ in length by 1.7 Å, which may affect the magnitude of the tunnelling current. However this magnitude is not used as a benchmark in this paper and small changes in the thickness of the director SAM are unlikely to influence asymmetry. The PSI in cyanobacteria has an asymmetric distribution of surface charges in the stroma and lumen sides (**Figure 2.2)**. Two thirds of all the charged surface residues are concentrated at the "top" of the complex; the stromal part or F_B electron acceptor side (**Figure 2.2**). This difference is likely to be what determines the preferred orientation of PSI during self-assembly on a modified gold surface. We

immobilized PSI on the substrates by drop casting from an aqueous buffer and incubating them (i.e. leaving them in contact) for two hours. We investigated each SAM topographically with AFM and electrically using CP-AFM. Also, we define the asymmetry of current transport (rectification ratio), R, as being the ratio I at positive to negative bias; R = |I (−)/I (+)| with respect to the wiring convention for CP-AFM (sample substrate is biased).

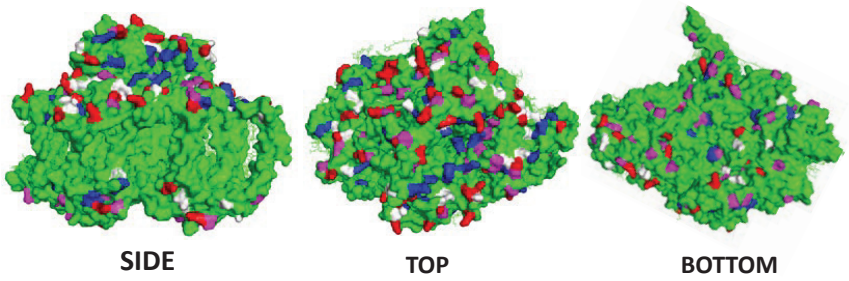

Figure 2.2 The structure of PSI protein complex extracted from *T. Elongatus* has more charges on the top (at Fe_4S_4) compared to the bottom (at P700 reaction centre). Two-thirds of all charges are concentrated on the top of the PSI protein complex, i.e. the part protruding to the stroma, which represents the internal chloroplast space. Amino acids are depicted as Lysine (red), Arginine (blue), Aspartic Acid (pink) and Glutamic Acid (white).

The recorded AFM height profile images show higher PSI coverage for 2ME than for MPS, with protein heights close to 6 nm on AuTS (**Figure 2.3**). This value is smaller than the 9 nm thickness derived from crystal structure data because these SAMs are measured under ambient, anhydrous conditions and contact with the AFM tip can compress them somewhat. We imaged individual PSI trimers within SAMs of PSI formed on both directing SAMs by AFM to determine the density. For 2ME, 853 PSI trimmers per μm^2 and for MPS, 723 trimers per μm^2 were measured. These different densities can be translated into surface coverage values. For 2ME and MPS coverages of 50% and 45% were calculated, respectively. Tapping mode imaging was performed at three different areas to account for surface inhomogeneity of SAMs. Next, CP-AFM electrical measurements were performed using the TUNA extension mode for AFM Multimode 8, where the conducting Pt/Ir coated doped Si probe was grounded and the gold surfaces with self-assembled linkers and PSI were biased with positive and negative voltages respectively for the I-V recording. The force applied to the CP-AFM probe was set as low as possible to minimise protein deformation during measuring, but was kept sufficiently high to record the tunnelling current via selected PSI protein complexes. A force of less than 10 nN was employed.

a) b)

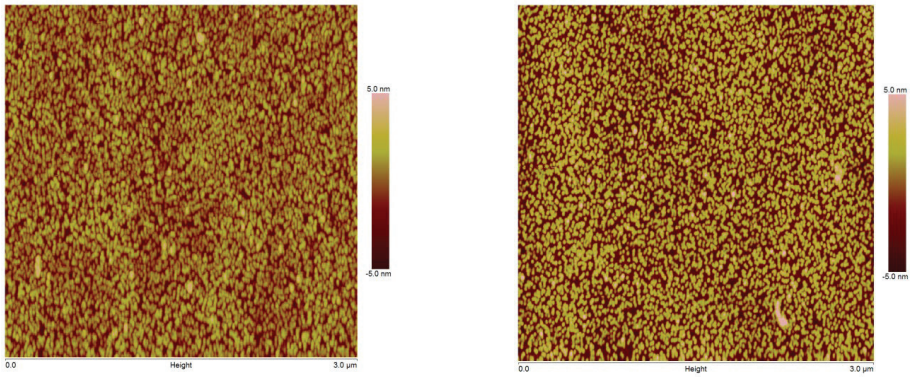

Figure 2.3. (a) and (b) an AFM image of the PSI coverage on the two surfaces modified with the corresponding linker molecules 2ME and MPS respectively.

These measurements allow to determine the orientation of single PSI trimmers according to **Figure 2.1b**[8-10]. The percentage PSI orientation defined by I-V rectification of diode-like curves (downwards, upwards and laterally) for each directing SAM molecule was determined by sampling 100 proteins in the dark. The results are summarized in **Table 2.1**. For 2ME, the majority of PSI is directed "downwards" (57%). In case of the other SAM molecule, MPS, 69% of the trimmers are oriented "upwards". The "parallel" orientation of PSI molecules is similar for both SAMs. The distribution ratio of I-V characteristics observed for 2ME is very similar to that measured previously in the literature for much smaller RCI[8-10].

Table 2.1. Percentage of average orientation of PSI depending on the different directing SAMs.

SAM	Down (%)	Parallel (%)	Up (%)
2ME	57	25	18
MPS	11	20	69

2.3 Electrical current rectification based on neutral PSI dipole moment

In the previous paragraph, the orientation of PSI was determined on two directors SAMs based on their rectification properties. Here, we study the mechanism of this rectification process. The PSI protein complex has a permanent dipole as a result of the composition of the amino acids[8]. The value of the PSI dipole moment can be calculated theoretically[18, 19] and in the case of the PSI trimer protein (used in our research) its direction was determined experimentally[20]. This dipole moment may result in the observed rectification as well (asymmetric recorded I-V curves) due to its internal electrical field, which is analogous to the rectification of well-studied self-assembled monolayers of surface-immobilized molecules with electron-withdrawing and electron-donating

groups (Donor-Acceptor)[21]. However, the implementation of the PSI dipole rectification model contradicts the *"evolutionary developed electron transport pathway"* model, which has been proposed previously[8-10]. The positive side of the PSI dipole is located at the P700 side, while the negative side is located at F_B side[20]. Therefore, the electrons need to travel against the dipole direction when moving on the electron acceptor chain after light illumination. That means two opposite rectification mechanisms are present in one PSI protein complex. If the current we measured by CP-AFM are due to the intrinsic dipole of PSI one would expect a charge transport mechanism relaying on the direct tunnelling between CP-AFM probe and Au substrate, which is temperature independent. In contrast, if the currents we measured follow the electron transport chain one would expect a transport via hopping on individual PSI redox centers. This process is temperature depended. Since temperature depended measurements with CP-AFM are hard to realize, EGaIn experiments were performed on the PSI trimer monolayers on the two director SAMs. These experiments were carried out in the group of Prof. R. Chiechi by Olga Castañeda Ocampo[22].

In **Figure 2.4a**, semi-logarithmic I-V (J-V, where J – is current density) curves are shown for the two PSI configurations with EGaIn as top electrode. The monolayer of PSI oriented "downwards" with the help of 2ME shows a higher rectification current than the protein layer directed "upwards" by MPS. In these experiments, the substrate was grounded. Both the EGaIn and the CP-AFM measurements can be directly compared because the PSI layers were prepared under identical conditions on the same surfaces. For this comparison, 50 I-V curves were recorded for both orientations with CP-AFM and averaged (**Figure 2.4b**). The resulting semi-logarithmic plots show the same trend as the EGaIn measurements[19, 16, 23, 24]. The 2ME directing SAM for PSI shows higher rectification than the MPS layer. Note that in this case the wiring was configured in such a way that the Pt/Ir tip was grounded. The fact that both techniques result in similar findings can also be seen when plotting the I-V curves for both directing SAMs in a conventional way (**Figure 2.4c and 2.4d**). The I-V curves of averaged CP-AFM measurements and macroscopic EGaIn experiments coincide for PSI on 2ME and MPS, respectively.

In the next step, the mechanism of electron transport through PSI trimers was investigated. Since CP-AFM does not allow recording of currents under large temperature variation EGaIn experiments were performed to address this question.

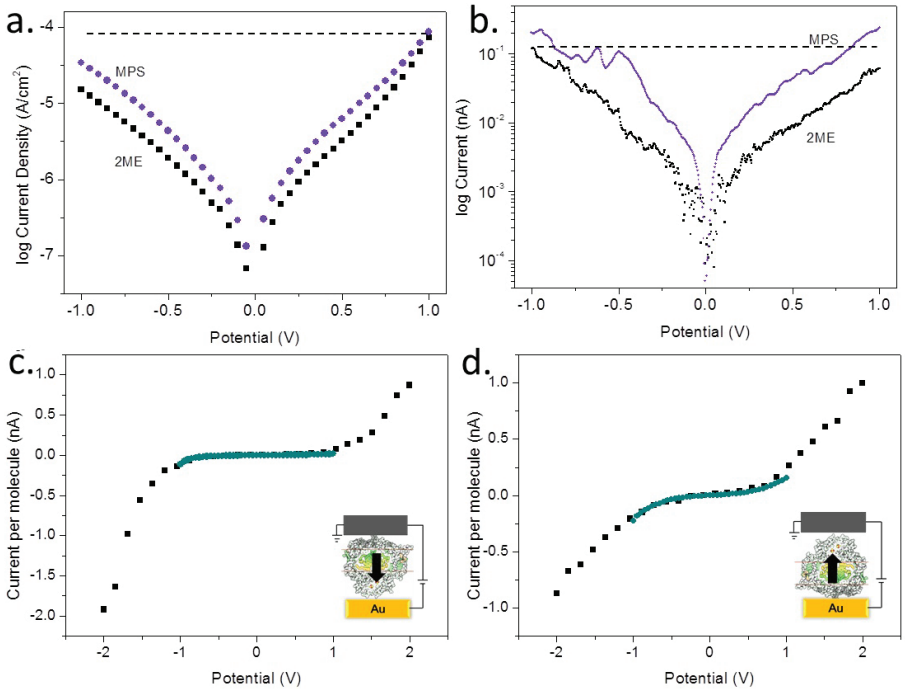

Figure 2.4. Top: Semi-log plots of current and current density versus voltage for junctions measured using EGaIn (a) and CP-AFM (b) for SAMs of PSI on MPS (purple) and 2ME (black). These data are plotted according to the normal wiring of each technique (see the Supporting Information for details). The horizontal, dashed lines are to guide the eye. Bottom: Per-complex J-V curves for SAMs of PSI on 2ME (c) and MPS (d) measured by CP-AFM (black squares) and EGaIn (green circles) plotted with respect to the standard wiring of CP-AFM (shown in the insets). Per-complex values of J for EGaIn were calculated using number densities of PSI measured by AFM and a correction factor for the difference between the measured and effective area of the EGaIn junctions[22].

Microfluidic devices fabricated following the protocols found in the literature were used to acquire J-V traces at different temperatures[16, 23]. The temperature was changed between 298 to 198 K. The plot of the ln |J| at ±0.50 V for PSI on both directing SAMs is described in **Figure 2.5**. It can be seem that the values of ln|J| do not vary over the broad chosen temperature range. These data are indicative for a charge transport mechanism that solely relies on tunnelling of electrons through PSI for both SAMs consisting of 2ME and MPS. Moreover, these results suggest that hopping is not involved in electron transport. On the other hand this means that the electrons do not travel via the redox elements of the electron transport chain.

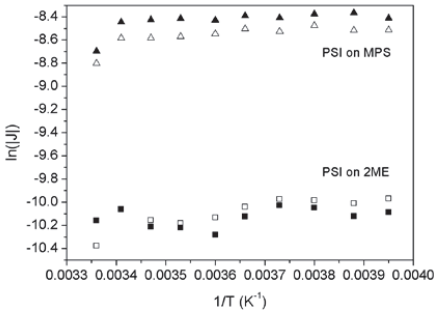

Figure 2.5. ln |J| at ±0.50 V as a function of inverse temperature for PSI on directing SAMs of MPS (triangles) and 2ME (squares). The solid symbols (▲,■) represent the positive bias (+0.50 V) and hollow (□, Δ) represent the negative bias (-0.50 V). The linearity indicates that the mechanism of charge transport is dominated by tunneling as no temperature dependence was measured.

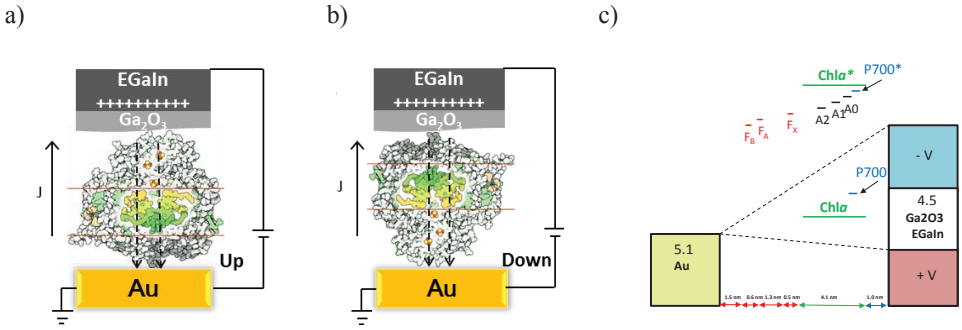

Figure 2.6. The direction of the electrical field that arises from the PSI dipole moment (dashed lines) within PSI-EGaIn devices, which are shown with EGaIn biased positively (with respect to the normal wiring of EGaIn). The direction of this field goes from positive to negative in the complex. (a) When PSI is oriented "up," the electric field from the applied bias opposes the internal electric field of the PSI complexes. (b) When PSI is oriented "down," the direction of the internal electric field is the same as the applied bias. Thus, this mechanism predicts that PSI in the down orientation will give higher values of *R*. (c) Energy level diagram across Au^{TS}-PSI(P700/F_B)//Ga_2O_3/EGaIn junctions. The barrier width is defined by the thickness of one oriented PSI complex, which is depicted in the "down" orientation with respect to the natural direction of electron flow. The green lines are the frontier orbital energies of the chlorophyll molecules, which are distributed evenly through the thickness of the PSI complex. The black lines represent the energies of the electron transport chain and their relative spatial positions. Based on the orientation of the electron transport chain, more current should flow when the EGaIn electrode is biased negatively than at the equivalent positive bias. That mechanism would translate into higher values of *R* when the complexes are oriented "up" (because this figure is drawn with respect to the wiring of EGaIn junctions; Figure 2.4 shows the data with respect to the wiring diagram of CP-AFM). The distances between co-factors were estimated with the software PyMOL from a crystal structure of PSI taken from the Protein Data Bank (1JB0).

After having determined the mechanism of charge transport through PSI, we can now make a statement about the absolute orientation of PSI on both directing SAMs. The permanent dipole of PSI that was theoretically calculated and experimentally determined by van Haeringen et al.[20] is characterized by a positive side at the P700 face while the negative side is located at the F_B face. The direction of the dipole of PSI is parallel to the C3-symmetry axis of PSI trimer. The electronic field of this dipole moment either enhances or opposes the total field that is generated by biasing the electrodes within the EGaIn experiments (**Figure 2.6a and 2.6b**). In the case of 2ME PSI is oriented in a "downwards" direction because we measure higher rectification current at positive voltage compared to MPS. On the other hand MPS orients the majority of PSI trimmers "upwards" since we detect lower rectification at positive voltage compared to 2ME. These results can be confirmed by looking at the energy levels of the electrodes, PSI and the redox centers of the electron transport chain (**Figure 2.6c**). This picture of the latter component was taken from Nakamura's observations[25]. It is clearly visible that during applying a bias of ±1V one does not reach the energy levels of the redox centers of PSI belonging to the electron transport chain (**Figure 2.6c**).

2.4 Conducting properties of PSI under illumination

After studying the electron transport through PSI in the dark and establishing a tunnelling mechanism not involving the electron transport chain, the question arises of how transport of the electrons occurs under illumination. Again CP-AFM measurements were performed to solve this question. A halogen lamp (400-700nm) was used as a single light source with a power of 10-30 $mW \cdot cm^{-2}$ for short time sample illumination when recording I-V curves. The same lamp and intensity was later employed in this thesis to follow oxygen consumption of PSI (see Chapter 5). For the acquisition of I-V curves by CP-AFM, a PSI trimer was selected by height image and the tip was placed on the top of the protein complex with a force of less than 10 nN. Firstly, trace and retrace curves were measured between -1.5 and +1.5 V. Subsequently, the lamp was switched on and the I-V curves on the same PSI trimer were recorded. For both directing SAMs, 2ME and MPS, and in the dark and under illumination 50 PSI trimmers were sampled individually resulting in a total of 200 I-V curves. For each configuration, the I-V curves were averaged and plotted (**Figure 2.7a**). In absence of light, the I-V curves adopt a S-shape indicating semiconducting behaviour. Thereby, similar rectification characteristics were observed as mentioned above (**Figure 2.4b**) for PSI directing SAMs consisting of 2ME and MPS. Once the light was switched on, the I-V curves changed significantly. A transition from semiconducting to ohmic was observed for both director SAMs. Under light illumination, a larger current for 2ME was measured than for MPS. After recording the I-V under illumination, the light was switched off and semiconducting S-shape I-V curves were restored.

These experiments clearly show that exciting the chlorophyll a molecules within PSI increases the current flow through the protein complex at both positive and negative bias. To put our results in perspective, we performed similar CP-AFM experiments with bovine serum albumin (BSA),

which represents a non-photoactive protein and does not contain any light-sensitive cofactors or any redox units. Again 50 I-Vs in light and in the dark were recorded on 2ME each. The averaged curves are plotted in **Figure 2.7b**. Asymmetric I-V curves were obtained for BSA indicating tunnelling through the protein scaffold. However, in contrast to PSI, the effect of illumination on BSA was negligible. Previously, scanning tunnelling microscopy (STM) and spectroscopy was performed on single light harvesting complex 2 (LHC 2), which does not exhibit an electron transport chain but possess light harvesting chlorophylls[26]. These measurements showed increased tunnelling current upon light irradiation, however, a complete transition from "semiconducting" to "ohmic" behaviour, as found in our experiments with PSI, was not observed[26]. We believe that the increase in tunnelling current under illumination and the appearance of ohmic behaviour are related to the increased generation of carriers within PSI under illumination in a dry state compared to the dark.

Due to the high amount of carriers generated by light within PSI the rectifying properties of the intrinsic dipole of PSI become less dominant and the conductivity solely gets determined by the external electric field. In this interpretation of the results, the contribution of electron acceptors of the electron transport chain of PSI is minor.

a) b)

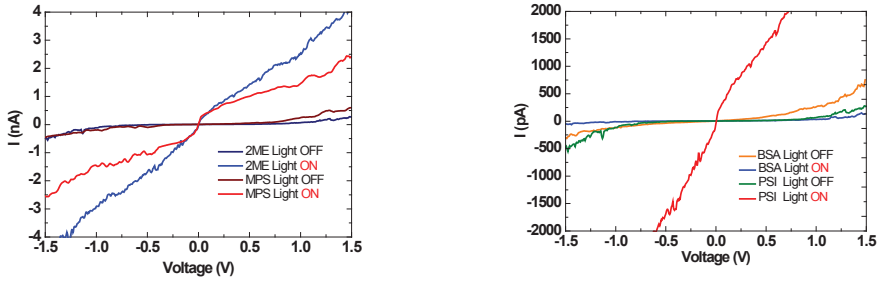

Figure 2.7 Averaged curves of CP-AFM on PSI protein complexes in dark conditions and under illumination on different SAMs. (a) The PSI protein complexes oriented on both linkers 2ME and MPS show enhanced currents for both cases. (b) The reference CP-AFM measurements with BSA proteins did not show an increase in current under illumination under the same measuring conditions as for PSI.

A similar ohmic behaviour of PSI under light illumination was observed in SNOM experiments with single PSI complex. Also the magnitude of absolute current was with 2 nA at ±1 V[6] comparable to the values measured here. While in SNOM[6] experiments an offset shift of 10 pA was detected that was ascribed to the photocurrent of a single PSI protein complex, here, we do not observed this photo-generated current with our CP-AFM setup.

2.5 Conclusions

In this chapter, were have immobilized PSI trimers on an Au-surface with two different linker molecules 2-mercaptoethanol (2ME) and 3-mercapto-1-propanesulfonate (MPS). These directing SAMs orient PSI trimers in on average opposite directions. 2ME forces the F_B side of PSI towards the surface while MPS induces the P700 side of PSI onto the substrate. This absolute orientation of PSI was determined by a set of different measurements. With CP-AFM the absolute orientation of PSI ratio of PSI protein complexes on the surface was determined by recording characteristic asymmetric I-V curves. These experiments were complemented by macroscopic EGaIn measurements on the same PSI monolayers. Temperature depended conductivity clearly demonstrated that the mechanism of electron transport is tunnelling. This result led to the conclusion that the electron acceptors of the PSI transport chain are not involved in transfer of electrons. For that reason the rectification must be due to the intrinsic dipole of PSI originating from the protein scaffold. It is noteworthy that the dipole induces opposite rectification as one would expect from the electron transport chain of PSI. Finally, we found that under illumination the conducting properties of PSI change completely compare to the dark. In absence of light, asymmetric I-V curves are diagnostic for the rectifying property of PSI. Under illumination, however, ohmic behaviour and a significantly larger conductivity are no longer determined by its intrinsic dipole.

2.6 Methods

Fabrication of monolayers. Immobilization of PSI, we immersed the substrates in a solution of 1mM 2-mercaptoethanol (2ME) or sodium 3-mercapto-1-propanesulfonate (MPS) to direct the PSI complexes to adopt a down or up orientation (F_B iron-sulfur cluster adjacent or away from substrate). The time of immersion was limited to 2 hours to avoid the formation of multilayers or aggregates. After this step, were rinsed the substrates with MQ water (MPS) or ethanol (2ME), dried them with nitrogen and incubated them in a previously prepared PSI solution. The PSI solution consisted of 1:1 in buffer A (20 mM HEPES (pH 7.5); 10 mM $MgCl_2$; 10 mM $CaCl_2$; 500 mM Mannitol with 0.05% DDM (n-Dodecyl-β-D-maltoside) for 2 h. They were then rinsed with MQ water and dried with nitrogen.

Monolayer Surface Characterization. We analyzed each substrate by AFM after each fabrication step: on the Au substrate after cleavage, after surface modification, and after incubation on PSI solution. We used the resulting images to measure the surface coverage of PSI. This analysis revealed a true surface coverage of up to 50%. This was calculated by knowing the diameter of the PSI trimer from TEM images and the coverage density for specific area. We obtained the AFM images with MultiMode 8 with ScanAsyst Microscope in tapping mode with TESP probes (Bruker) with spring constant k = 42 $N \cdot m^{-1}$, resonance frequency f = 320–410 kHz and tip radius of less than 10 nm. The scan rate and resolution were 1 Hz and 640 lines/sample respectively. We analysed the AFM images with the software NanoScopeAnalysis 1.2 from Bruker. We studied the conductivity of the immobilized PSI on the two orienting monolayers with AFM Tunneling

Atomic Force Microscopy (TUNA) contact mode with a conducting probe. This mode was applied for electrical characterisation of single (trimer) PSI complex with Pt/Ir coated Si n-type probe (APPNano), spring constant k = 0.02-0.8 $N \cdot m^{-1}$, resonance frequency f = 5-25 kHz and tip radius less than 30 nm with contact resistance of 0.01-0.025 ohm/cm. Statistic data was performed over 100 independent measured points for each orienting SAM. The applied force to CP-AFM conducting probe on top of PSI was started from low and step-by-step increased to reach contacting for I-V recording. This approach was used for each measurement point with forces less than 10 nN.

2.7 References

1. Mershin, A. et al. Self-assembled photosystem-I biophotovoltaics on nanostructured TiO2 and ZnO. *Sci. Rep.* **2** (2012).

2. Iwuchukwu, I.J. et al. Self-organized photosynthetic nanoparticle for cell-free hydrogen production. *Nat. Nanotechnol*. **5**, 73-79 (2010).

3. Carmeli, I. et al. Spatial modulation of light transmission through a single microcavity by coupling of photosynthetic complex excitations to surface plasmons. *Nat. Commun.* **6** (2015).

4. Golbeck, J.H. Structure and Function of Photosystem-I. *Annu. Rev. Plant. Phys.* **43**, 293-324 (1992).

5. Das, R. et al. Integration of photosynthetic protein molecular complexes in solid-state electronic devices. *Nano Lett.* **4**, 1079-1083 (2004).

6. Gerster, D. et al. Photocurrent of a single photosynthetic protein. *Nat. Nanotechnol*. **7**, 673-676 (2012).

7. Carmeli, I., Frolov, L., Carmeli, C. & Richter, S. Photovoltaic activity of photosystem I-based self-assembled monolayer. *J. Am. Chem. Soc.* **129**, 12352(2007).

8. Lee, I., Lee, J.W., Warmack, R.J., Allison, D.P. & Greenbaum, E. Molecular Electronics of a Single Photosystem-I Reaction-Center - Studies with Scanning-Tunneling-Microscopy and Spectroscopy. *P. Natl. Acad. Sci. USA* **92**, 1965-1969 (1995).

9. Lee, I., Lee, J.W. & Greenbaum, E. Biomolecular electronics: Vectorial arrays of photosynthetic reaction centers. *Phys. Rev. Lett.* **79**, 3294-3297 (1997).

10. Lee, J.W., Lee, I. & Greenbaum, E. Platinization: A novel technique to anchor photosystem I reaction centres onto a metal surface at biological temperature and pH. *Biosens. Bioelectron.* **11**, 375-387 (1996).

11. Stamouli, A., Frenken, J.W.M., Oosterkamp, T.H., Cogdell, R.J. & Aartsma, T.J. The electron conduction of photosynthetic protein complexes embedded in a membrane. *FEBS Lett.* **560**, 109-114 (2004).

12. Mikayama, T. et al. The Electronic Behavior of a Photosynthetic Reaction Center Monitored by Conductive Atomic Force Microscopy. *J. Nanosci. Nanotechno.* **9**, 97-107 (2009).

13. Frolov, L., Rosenwaks, Y., Carmeli, C. & Carmeli, I. Fabrication of a photoelectronic device by direct chemical binding of the photosynthetic reaction center protein to metal surfaces. *Adv. Mater.* **17**, 2434 (2005).

14. Reiss, B.D., Hanson, D.K. & Firestone, M.A. Evaluation of the photosynthetic reaction center protein for potential use as a bioelectronic circuit element. *Biotechnol. Progr.* **23**, 985-989 (2007).

15. Chiechi, R.C., Weiss, E.A., Dickey, M.D. & Whitesides, G.M. Eutectic gallium-indium (EGaIn): A moldable liquid metal for electrical characterization of self-assembled monolayers. *Angew. Chem. Int. Edit.* **47**, 142-144 (2008).

16. Dickey, M.D. et al. Eutectic gallium-indium (EGaIn): A liquid metal alloy for the formation of stable structures in microchannels at room temperature. *Adv. Funct. Mater.* **18**, 1097-1104 (2008).

17. Yamanoi, Y., Terasaki, N., Miyachi, M., Inoue, Y. & Nishihara, H. Enhanced photocurrent production by photosystem I with modified viologen derivatives. *Thin Solid Films* **520**, 5123-5127 (2012).

18. Felder, C.E., Prilusky, J., Silman, I. & Sussman, J.L. A server and database for dipole moments of proteins. *Nucleic Acids Res.* **35**, W512-W521 (2007).

19. Antosiewicz, J. & Porschke, D. Electrostatics of Hemoglobins from Measurements of the Electric Dichroism and Computer-Simulations. *Biophys. J.* **68**, 655-664 (1995).

20. Vanhaeringen, B. et al. Simultaneous Measurement of Electric Birefringence and Dichroism - a Study on Photosystem-1 Particles. *Biophys. J.* **67**, 411-417 (1994).

21. de Boer, B., Hadipour, A., Mandoc, M.M., van Woudenbergh, T. & Blom, P.W.M. Tuning of metal work functions with self-assembled monolayers. *Adv. Mater.* **17**, 621 (2005).

22. Castaneda Ocampo, O.E. et al. Mechanism of Orientation-Dependent Asymmetric Charge Transport in Tunneling Junctions Comprising Photosystem I. *J. Am. Chem. Soc.* **137**, 8419-8427 (2015).

23. Nijhuis, C.A., Reus, W.F., Barber, J.R., Dickey, M.D. & Whitesides, G.M. Charge Transport and Rectification in Arrays of SAM-Based Tunneling Junctions. *Nano Lett.* **10**, 3611-3619 (2010).

24. So, J.H. & Dickey, M.D. Inherently aligned microfluidic electrodes composed of liquid metal. *Lab Chip* **11**, 905-911 (2011).

25. Nakamura, A., Suzawa, T., Kato, Y. & Watanabe, T. Species Dependence of the Redox Potential of the Primary Electron Donor P700 in Photosystem I of Oxygenic Photosynthetic Organisms Revealed by Spectroelectrochemistry. *Plant Cell Physiol.* **52**, 815-823 (2011).

26. Lukins, P.B. Single-molecule electron tunneling spectroscopy of the higher plant light-harvesting complex LHC II. *Biochem. Bioph. Res. Co.* **256**, 288-292 (1999).